



Inkjet-printed colorimetric indicators from the peels of red pitaya and Kyoho grape for the detection of food spoilage gases

Tianxi Gong^a, Xiaoyu Luo^{a,b,*} 

^a Food Science and Technology Program, Beijing Normal–Hong Kong Baptist University, Zhuhai, Guangdong, 519087, China

^b Guangdong Provincial Key Laboratory of Interdisciplinary Research and Application for Data Science, Beijing Normal–Hong Kong Baptist University, Zhuhai, Guangdong, 519087, China

ARTICLE INFO

Handling Editor: Dr. Maria Corradini

Keywords:

Intelligent packaging
Colorimetric indicator
Anthocyanin
Betacyanin
Fruit waste

ABSTRACT

The development of intelligent packaging materials can be alternative means to monitor food freshness and showcase real-time quality decline during storage. Colorimetric indicators are commonly employed as such examples due to their capability to exhibit chemically-responsive color changes triggered by the in-package headspace change during food deterioration. Different food-grade indicator dyes or pigments were investigated in literature, but one challenge was to incorporate the colorant into packaging materials with easy manipulation of indicator compositions. In this study, betanin extracted from red pitaya peel and anthocyanin extracted from Kyoho grape peel were developed into inks and subsequently printed as colorimetric indicators through piezoelectric inkjet printing. The formulated ink solution containing indicator compounds exhibited Newtonian fluid characteristic and was confirmed as printable fluid. The developed indicators showed detectable color responses upon the exposure of increasing levels of different food volatile gases including acetic acid, butyric acid, trimethylamine, ammonia and hexanoic acid. For each gas analyte present at low and high doses, the indicator's color responses can be differentiated by conducting the principal component analysis and hierarchical cluster analysis, with high sensitivity. A preliminary study on seafood freshness monitoring was conducted and visible color changes were observed during shrimp deterioration.

1. Introduction

Food spoilage is common to all perishable foods, involving fresh meat, seafoods, dairy foods, fruits and vegetables, resulted in quality deterioration and subsequent food waste generation (Luo et al., 2022). To accurately evaluate the shelf-life of specific packaged commodity, analytical instruments can be employed, such as gas or liquid chromatographs for chemical metabolite detection and electronic nose/tongue for undesirable aroma/taste compound analysis, but they are usually time-consuming, laborious, or requiring expertise and personnel (Kalpana et al., 2019; Mehrzad et al., 2024). Hence, the development of a fast, low-cost, and sensitive method that can showcase food quality is a promising alternative (Chen et al., 2020). One of these advanced alternative approaches is intelligent packaging, which can indicate the real-time food quality information via deliberate incorporation of indicator or bar code onto the packaging substrate (Cheng et al., 2022; Zhang and Lim, 2016). The developed intelligent packaging materials can enhance the communication and convenience function of a food

package, thereby involving the interactions between the product and all food supply participants and providing dynamic information of the product (Luo et al., 2022; Yam et al., 2005). Therefore, as a supplementary method, the formulation and utilization of intelligent packaging materials is expected to aid food quality detection and traceability, in order to tackle food wastage in the long run.

For commercial packaging substrates, printing is a common method for food labelling and advertisements, including gravure, flexographic, lithographic, screen and digital printing techniques (Robertson, 2016). While the former four are conventional printing methods, inkjet printing belongs to the digital printing, which is a non-contact process that allows for rapid ink deposition with high accuracy and precision (Luo, 2022). There are two forms of inkjet printing: continuous inkjet (CIJ) printing that eject ink drops continuously, and drop-on-demand (DOD) ink-jet printing that can be controlled with ink jetting per printing demand (Derby, 2010).

Since a number of intelligent packaging materials are to be formulated from solutions or suspensions, inkjet printing can be a promising

* Corresponding author. Food Science and Technology Program, Beijing Normal–Hong Kong Baptist University, Zhuhai, Guangdong, 519087, China.
E-mail address: xiaoyuluo@uic.edu.cn (X. Luo).

Table 1
Physical properties and Z value of the formulated colorimetric inks.

Ink colorant	Density ($\text{g}\cdot\text{cm}^{-3}$)	Surface tension ($\text{mN}\cdot\text{m}^{-1}$)	Dynamic viscosity ($\text{mPa}\cdot\text{s}$)	Z value
Anthocyanin	0.93	9.38	1.97	5.65
Betacyanin	0.96	9.68	2.32	4.97

method for their fabrication of these liquids on food packages. A few studies have demonstrated the potential of inkjet-printed intelligent packaging material, even the application in food systems is still scarce. For example, [Tasangtong et al. \(2023\)](#) developed a paper-based colorimetric indicator to detect the formaldehyde content in foods. [Soni et al., 2024](#) prepared inkjet-printed conductive graphene nanocomposites on light polydimethylsiloxane in order to develop a low-cost temperature sensor (2024). The combination of mobile phones and inkjet-printed colorimetric cards were studied by [Patel et al. \(2022\)](#) in order to detect pesticide residues in food. In another study, an inkjet-printed film was used as an oxygen sensor to showcase detectable color changes in modified atmospheric products ([Fernández-Ramos et al., 2021](#)). From our previous research outputs, we employed DOD piezoelectric inkjet printing to generate sulfonaphthalein dye-based colorimetric indicators, which did show discriminative capacity for volatile amines and can be used to predict fish deterioration based on their sensitive

chemical-responsive color response ([Luo and Lim, 2020a](#); [Luo et al., 2021](#)).

When food deteriorates, with self-digestion and growth of microorganisms, food components are gradually decomposed, resulted in different metabolites, which can be targeted by intelligent packaging materials to assess food freshness. For instance, in fish and seafood products, trimethylamine (TMA), ammonia (NH_3) and dimethylamine are the characteristic substances that cause the smelly fishy odor imparting spoilage. These volatile amines are mainly produced by *Pseudomonas* spp. and *Shewanella putrefaciens* involved in the degradation of nitrogen compounds contained in food ([Pacquit et al., 2007](#)). In fruits and fermented foods, prolonged storage leads to the unpleasant sour taste triggered by the short-chain fatty acids, such as butyric and hexanoic acid, which are produced by carbohydrate degradation via the activities of *Lactobacillus*, *Clostridium kluveri* and *Clostridium butyricum* ([André et al., 2017](#); [San-Valero et al., 2019](#)). Acetic acid is a common food spoilage metabolite produced by acetic acid bacteria in various foods and imparts an intense sour smell ([Saichana et al., 2015](#)). Since these iconic degradation products from food spoilage have been studied in literature, it is feasible to develop dye- or pigment-based indicators through inkjet printing, so that the level of spoilage metabolites can be well-correlated with indicator's color change in the visible range.

Natural pigments are prevalent from diverse plant, animal and algae sources, involving carotenoids, flavonoids, alkaloids, indigoids, and so

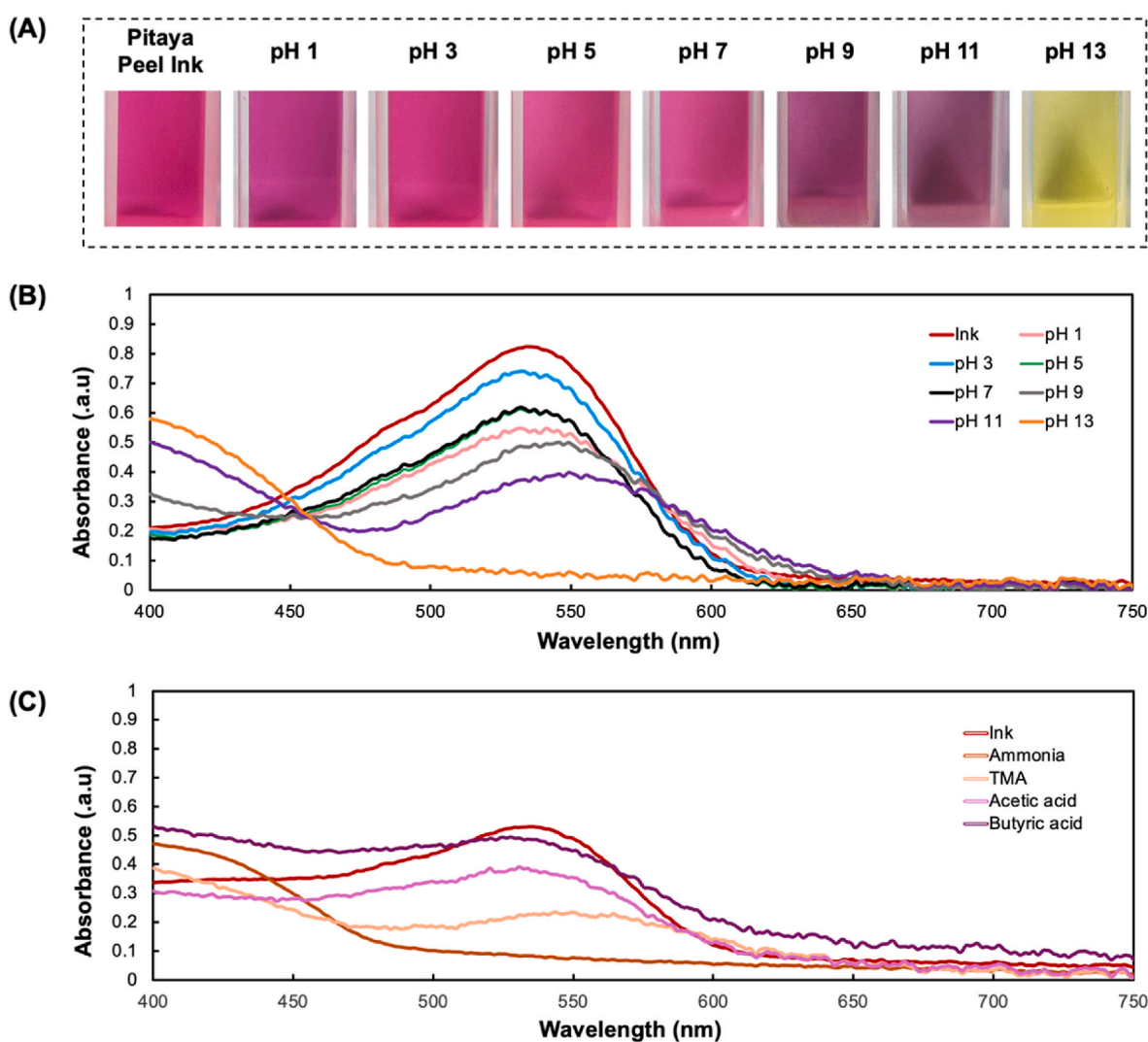


Fig. 1. The pH sensitivity of red pitaya peel ink: (A) color response at various pH conditions; (B) visible absorption spectra of the ink at different pH conditions (1, 3, 5, 7, 9, 11, and 13); and (C) visible absorption spectra of the ink exposed to ammonia, TMA, acetic acid and butyric acid.

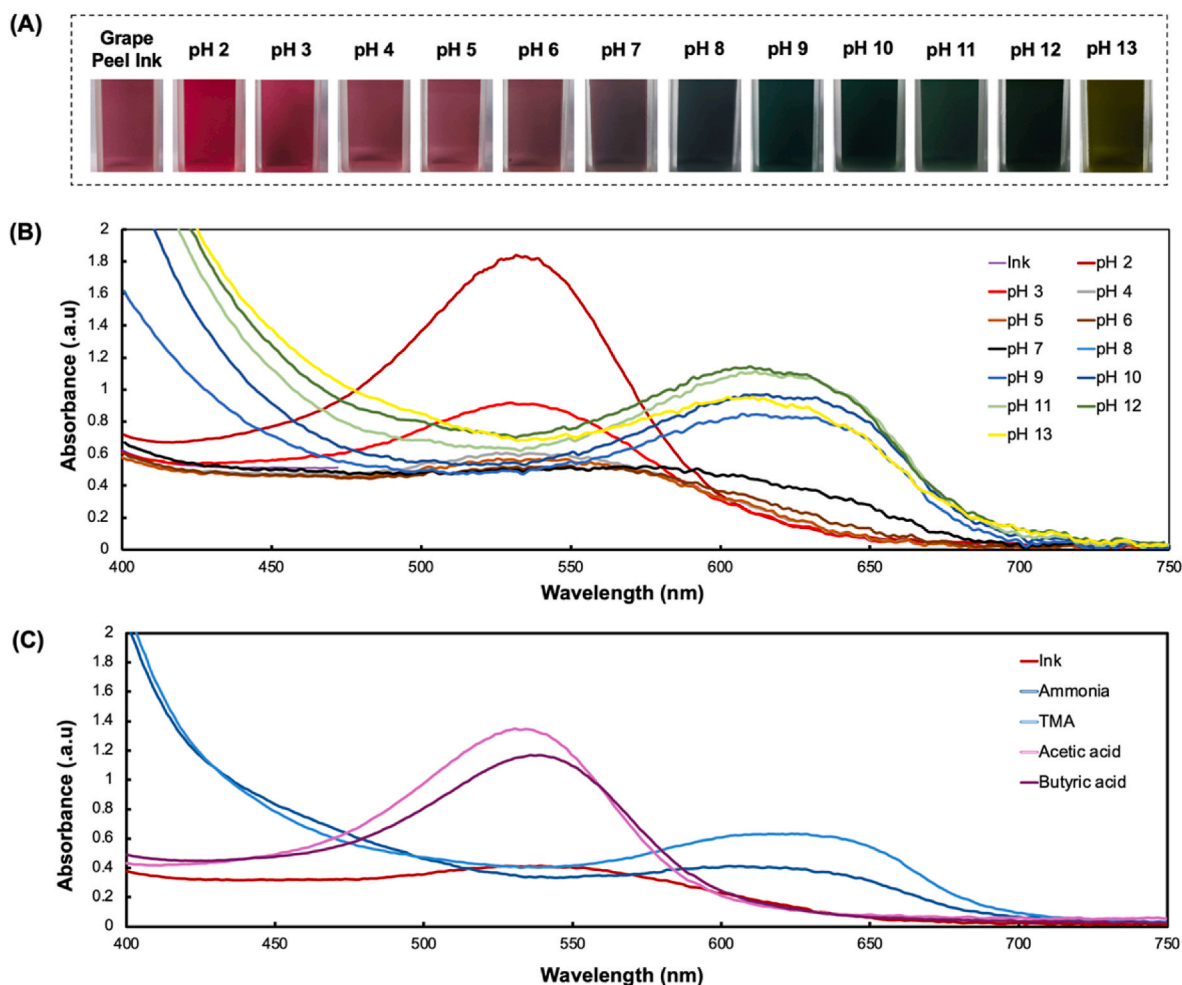


Fig. 2. The pH sensitivity of grape peel ink: (A) color response at various pH conditions; (B) visible absorption spectra of the ink at different pH conditions (pH 2–13); and (C) visible absorption spectra of the ink exposed to ammonia, TMA, acetic acid and butyric acid.

on (Rodríguez-Mena et al., 2023; Yu et al., 2024). Anthocyanin is a natural water-soluble pigment that is widely found in purple/red plants, such as grape, blueberry, and red cabbage. Anthocyanins have excellent antioxidant properties and are often added to food as a natural coloring agent (Chen et al., 2020; Stafford, 1994). The pH-responsive color change of anthocyanin makes it a compatible indicator compounds for intelligent packaging. Specifically, the reversible color change of anthocyanins are triggered by the protonation or deprotonation of the phenol groups. Under acidic conditions, the predominant form is flavone cation imparting reddish color; when the pH constantly increases, the hydration of flavone cation and proton transfer occurs. After flavone cation hydration, colorless carbinol pseudobase is formed (pH 4–6), and the ring structure opens with yellow chalcone formation when the pH becomes slightly alkaline (Kossyvakı et al., 2022; Yu et al., 2024). Betalain is a natural water-soluble nitrogen-containing pigment, composed of two main components, namely betacyanins with maximum absorption at 538 nm and betaxanthins with maximum absorption at 480 nm (Stafford, 1994). Betalamic acid is a chromophore common to all betalain pigments, and the type of residues added to betalamic acid determines the pigment classification of betacyanin or betaxanthin (De Azeredo et al., 2009; Fu et al., 2020). In alkaline environment or heat treatment, red betacyanin is easily hydrolyzed to become yellow betaxanthin and colorless cyclic dopa 5-O- β -glucoside (Herbach et al., 2006), so betalains are also capable of inducing pH-sensitive color changes.

Unlike previous studies using single pigments as an indicator of food freshness, in the present study, we aim to formulate the indicator

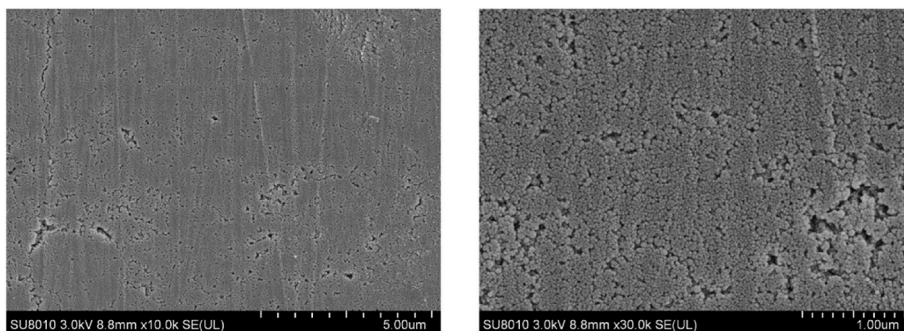
solution by blending the printing inks made from betanins and anthocyanins. Colorimetric indicators developed from two types of pigments are advantageous in providing a broader color-response spectrum, where betanins change their color mainly in alkaline conditions and anthocyanins can provide considerable color changes in acidic to slightly alkaline pH conditions. The use of pitaya and grape peels as raw materials for pigment extraction can significantly reduce the cost of intelligent packaging development and allow for food waste re-utilization. Therefore, this study aims to extract natural pigments from fruit peels, prepare printable inks, and develop inkjet-printed natural colorimetric indicators for the detection of food spoilage gases. The color-change mechanism and printability of the prepared inks are investigated, and the performance on indicator's color response to different volatile gases are evaluated, followed by a preliminary study on monitoring shrimp freshness.

2. Materials and methods

2.1. Materials

Fresh red pitayas (*Hylocereus polyrhizus*) and grapes (*Vitis labrusca* 'Kyoho') were purchased from a local grocery store, transported to the laboratory with chilled packaging by ice, and stored at refrigerated temperature for further usage. TMA (31–35 wt% in ethanol, 4.2 M, contains toluene as stabilizer), ammonium hydroxide (35 wt%), acetic acid, butyric acid, hexanoic acid, and Pectinex Ultra SP-L obtained from *Aspergillus aculeatus* were all purchased from Sigma Aldrich (Merck

(A) Blank photo paper



(B) Indicator 100M/100C printed on photo paper

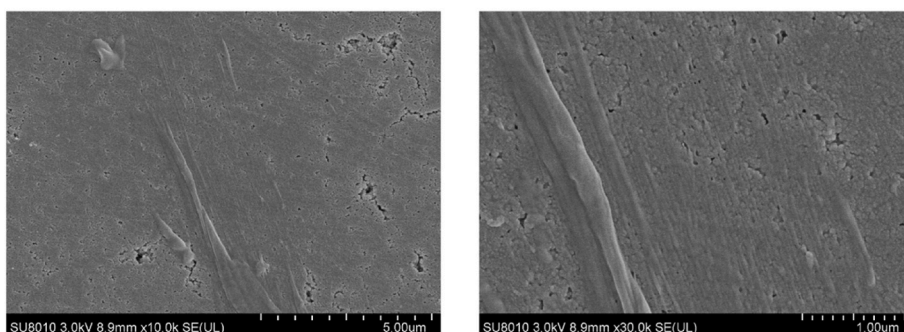


Fig. 3. SEM micrographs of (A) blank photo paper and (B) 100M/100C indicator.

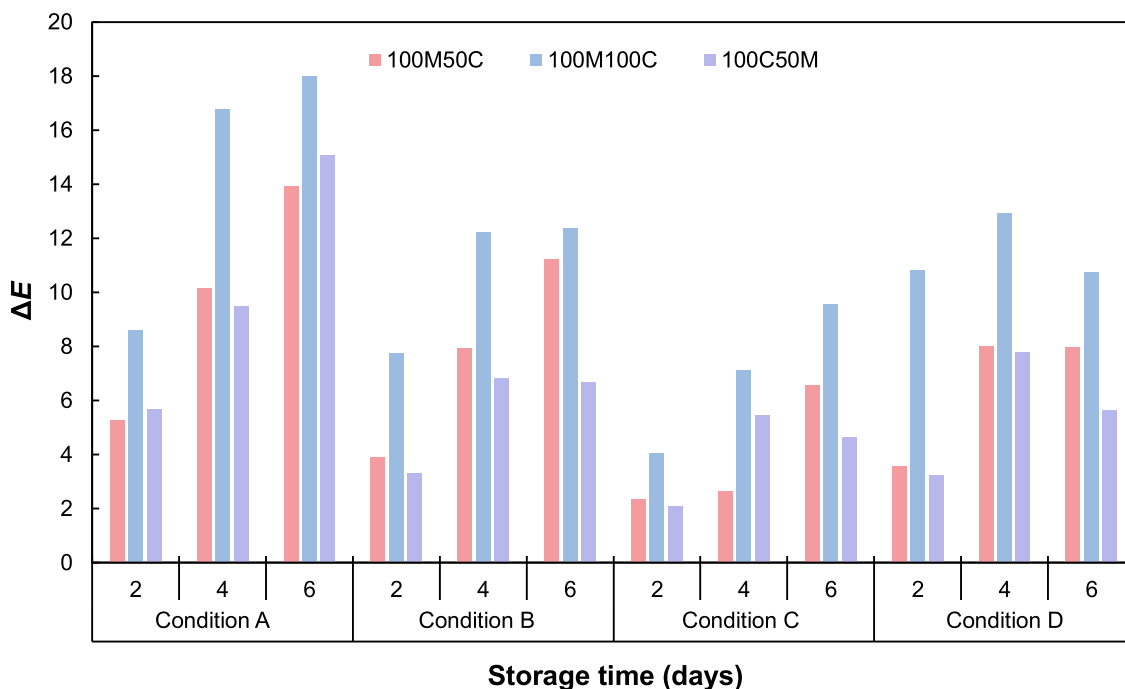


Fig. 4. Comparison of total color changes (ΔE) of the three indicators stored under different conditions for 6 days, where condition A represents light and oxygen exposure, condition B indicates represents, condition C represents dark and vacuum, and condition D represents dark and oxygen.

KGaA, Shanghai, China). Glycerol, isopropanol, citric acid, ethanol were purchased from Macklin (Huatong, Shanghai, China). Polypropylene containers (100 mL, with lids) were purchased from Chengda Department Ltd. (Ningbo, China). The reagents were directly used as received

without purification.

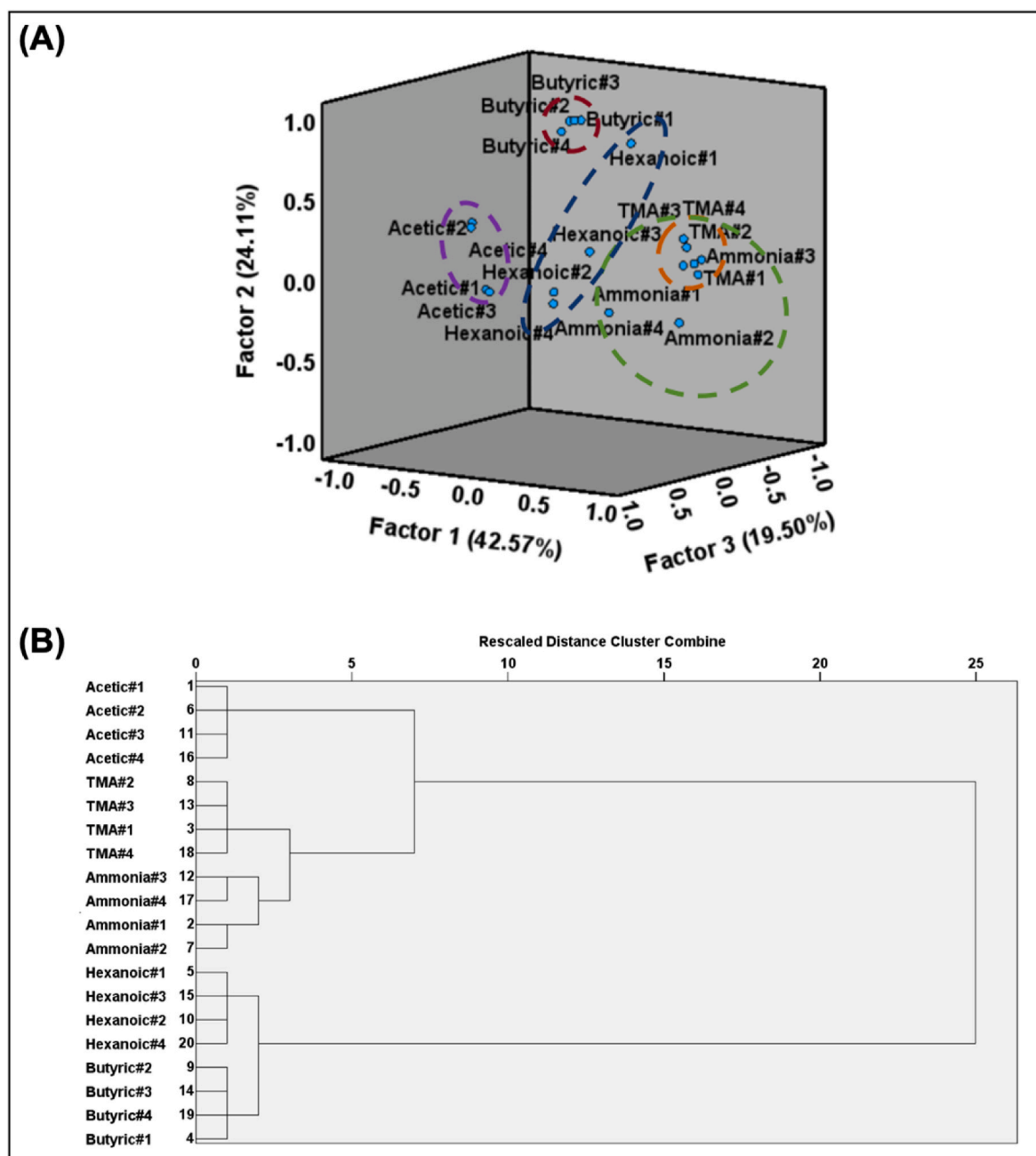


Fig. 5. (A) Principal component analysis plot and (B) hierarchical cluster analysis dendrogram for the colorimetric detection of five different gas analytes (ammonia, acetic acid, TMA, butyric acid, and hexanoic acid) at 25 °C.

2.2. Pigment extraction

2.2.1. Betanin extraction from red pitaya peel

The extraction steps were accomplished through the enzyme-assisted extraction method based on the study by Phan Van et al. (2020), with modifications. Fresh pitaya peel was dried in the oven for 12 h at 60 °C. For every trial, 50 g dried red pitaya peel and 500 mL distilled water were placed into an 1 L Erlenmeyer flask, followed by the addition of Pectinex Ultra SP-L (1.75 % v/w of fruit peel dry weight basis) with gentle and constant stirring. The mixture was then transferred into rotary evaporator with 20-min rotation at 35 °C and 150 rpm. The enzyme in the mixture was then deactivated by hot water bath at 90 °C for 1 min. The mixture was vacuum filtered to remove solid impurities and the extracted pigments were left in the remaining clear liquid. The betanin-rich liquid was then placed in a vacuum oven (10 Pa) and dried

at 40 °C for 24 h to produce the concentrated pitaya pigment extract (CPPE) for further use. The betacyanin content in CPPE was 4.48 mg/g dried pitaya peel.

2.2.2. Anthocyanin extraction from kyoho grape peel

The extraction of anthocyanins from Kyoho grape peel was referred to the study by Chen et al., in 2020, with modifications. Fresh grape peel was dried in the oven for 4 h at 40 °C. For each trial of anthocyanin extraction, 20 g of dried grape peel was blended with 400 mL ethanol (50 % v/v) were placed in a beaker. Citric acid (2 % w/v of peel and ethanol mixture) was added to the mixture to retain pigment stability. The mixture was then transferred to a water bath at 60 °C operated for 1 h. After cooling, the pigments were vacuum filtered in the clear liquid with red-purplish color. To increase anthocyanin content, the collected liquid extract stored in the vacuum oven and dried at 40 °C for 24 h to

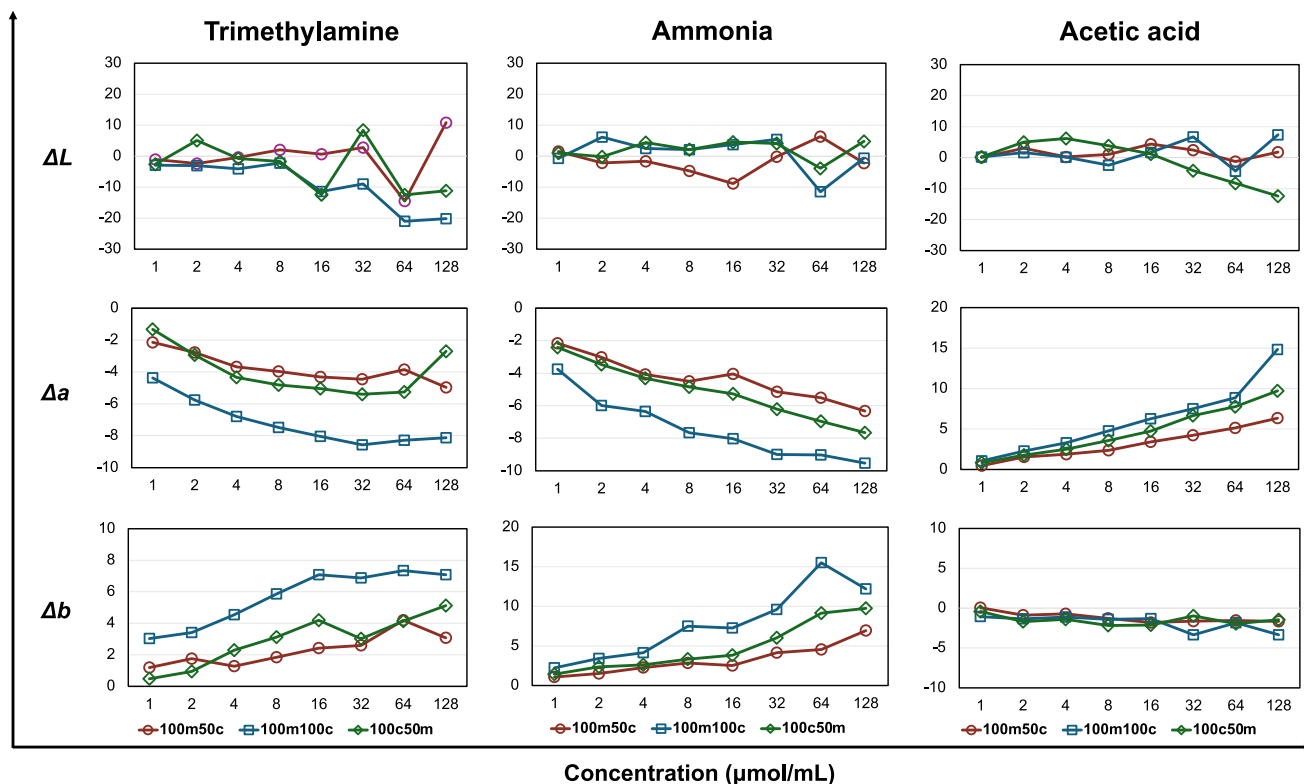


Fig. 6. Change of L^* , a^* , b^* values of the prepared three indicators (100M/50C, 100M/100C, and 100C/50 M) upon the exposure to different levels (1–128 $\mu\text{mol/mL}$) of TMA, ammonia, and acetic acid.

produce the concentrated grape pigment extract (CGPE). The anthocyanin concentration in the extract was 3.42 mg/g dried grape peel.

2.3. Printing ink formulation

The procedure of printing ink formulation is based on our preliminary trials for successful ink preparation. To prepare the printing ink, 10 g of CPPE or CGPE was diluted in 10 mL distilled water with constant stirring, with the subsequent addition of 10 mL ethanol (95 %) and glycerol (5 % w/w). The prepared mixture was centrifuged at 8000 rpm for 10 min at 4 °C. After centrifugation, the supernatant was obtained and transferred to a brown glass bottle, and stored at dark and dry conditions for further use as the printing ink.

2.4. Ink pigment determination

2.4.1. Betacyanin determination

The total betacyanin content in the prepared ink was determined based on the method described by Qin et al. (2020). The ink made from concentrated betanin-rich liquid was diluted with deionized water, and the absorbance of the dilute solution at 538 nm was determined by a UV-Vis spectrophotometer (Mettler Toledo, Switzerland). The total betacyanin content was calculated by Equation (1) and expressed as mg betacyanin per mL of ink:

$$\text{Betacyanin content (mg/mL)} = \frac{\text{DF} \times A \times \text{MW}}{\epsilon \times L} \quad (1)$$

where DF is the dilution factor, A is the absorbance at 538 nm, L is path length of cuvette (1 cm). MW (550 g mol^{-1}) and ϵ (65,000 $\text{L mol}^{-1}\cdot\text{cm}^{-1}$) represent the molecular weight and molar extinction coefficient of betanin, respectively.

2.4.2. Anthocyanin determination

Total anthocyanins in the prepared ink were determined according to the pH differential spectroscopic method (Etxabide et al., 2021). The ink made from CGPE was diluted by two different buffers: 0.025 M potassium chloride (pH 1.0) and 0.4 M sodium acetate (pH 4.5). After incubation at room temperature for 30 min, the absorbance of the solution at 510 nm and 700 nm was measured by UV-Vis spectrophotometer. The total anthocyanin content was calculated by Equations (2) and (3), and expressed as mg anthocyanin per mL of ink.

$$A = (A_{510} - A_{700})_{\text{pH}1.0} - (A_{510} - A_{700})_{\text{pH}4.5} \quad (2)$$

$$\text{Anthocyanin content (mg/mL)} = \frac{\text{DF} \times A \times \text{MW}}{\epsilon \times L} \quad (3)$$

where DF is dilution factor, A is the absorbance difference between 510 nm and 700 nm, L is the path length of cuvette (1 cm). MW (445 g mol^{-1}) and ϵ (15,600 $\text{L mol}^{-1}\cdot\text{cm}^{-1}$) represent the molecular weight and molar extinction coefficient of betanin, respectively.

2.5. Printing ink characterization

2.5.1. Printability test

According to our previous work (Luo and Lim, 2020a), the printability of the prepared ink can be assessed by Z value, which can be calculated based on Equation (4):

$$Z = \frac{\sqrt{\gamma \rho a}}{\eta} \quad (4)$$

where γ , ρ , and η are respectively the surface tension ($\text{mN}\cdot\text{m}^{-1}$), density ($\text{g}\cdot\text{mL}^{-1}$) and dynamic viscosity ($\text{mPa}\cdot\text{s}$) of the formulated ink, and a is the characteristic distance, explicitly the diameter of the ink droplet. The physical properties, γ , ρ , and η were measured at room temperature

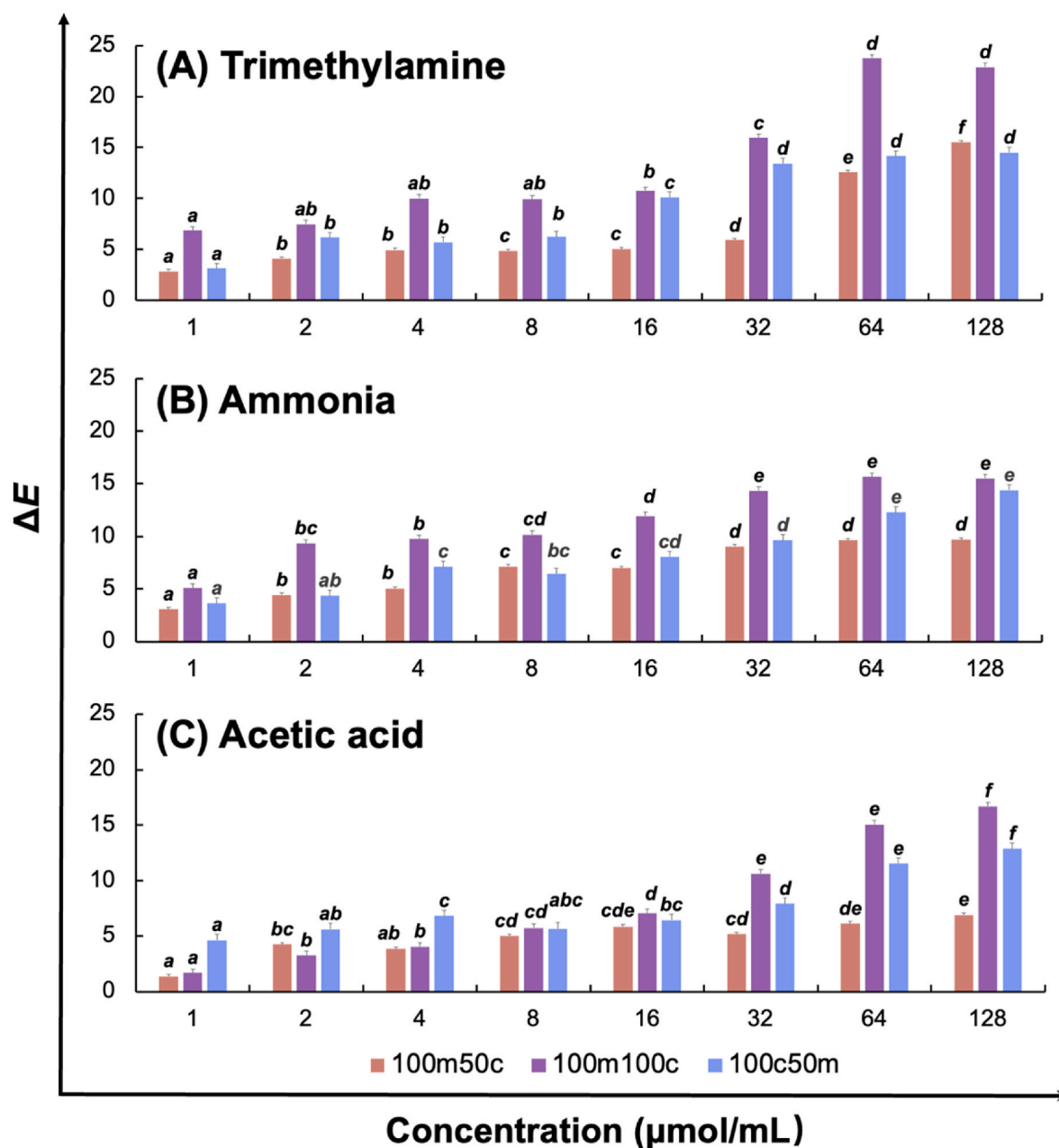


Fig. 7. Comparison of the three indicators' overall color changes (ΔE) for the exposure to (A) TMA, (B) ammonia and (C) acetic acid. The different letters on top of each error bar represents significant difference of color change between different gas concentrations of the same indicator ($p < 0.05$).

by surface tensiometer (DSA100, KRUSS, German), analytical balance, and rheometer (DHR-1, TA, USA) respectively. The dynamic viscosity of each ink was determined using a 2° steel cone plate (60-mm diameter; 52 μm gap) over the shear range of 10–1000 s⁻¹. The characteristic length a is estimated from the volume of the smallest printed droplet provided in the printer user's manual.

2.5.2. Ink pH sensitivity

The previously prepared CPPE and CGPE inks were diluted with Mill-Q water (1:19 v/v) respectively, and subsequently adjusted to various pH levels between 1 and 13 through the addition of 2 M hydrochloric acid or sodium hydroxide solution. The ink's color appearance and absorbance spectra in visible range were recorded by a digital camera and the UV-Vis spectrophotometer.

2.6. Indicator preparation by piezoelectric inkjet printing

The colorimetric indicators were developed by refilling the original cartridge of a piezoelectric inkjet printer (Epson XP-2100) with previously formulated betanin and anthocyanin inks, followed by the printing on photo papers. Before each run of ink replacement, the printer nozzle was rinsed by the cleaning solution made from ethanol, water, and isopropanol with 2:1:2 (v/v/v) ratio. The inks of CPPE and CGPE were transferred into the Yellow (Y) and Magenta (M) respectively to replace the original commercial inks. After the ink-filled cartridges were assembled, the printer's default "Print Check" function was performed to ensure smooth ink ejection and printing consistency. The printed indicator pattern was obtained through a Microsoft Power Point design as a 1 cm × 2 cm rectangular shape with C/M/Y/K value of 100/50/100/0, 100/100/0/0, 50/100/0/0, further denoted as indicator "50M/100C", "100M/100C", and "100M/50C" respectively.

Table 2

Limit of detection (LOD) and limit of quantification (LOQ) for the detection of acetic acid, ammonia and trimethylamine (TMA).

Indicator	Gas analyte	Equation	R ²	LOD (μmol/mL)	LOQ (μmol/mL)
100M50C	Acetic acid	y = 0.6319x + 2.6135	0.8666	0.95	2.81
	Ammonia	y = 0.9645x + 3.6308	0.8937	1.47	4.43
	TMA	y = 0.9272x + 1.7124	0.9579	1.24	3.72
100M100C	Acetic acid	y = 2.2019x + 0.3208	0.9432	0.48	1.44
	Ammonia	y = 1.4272x + 6.4779	0.9308	0.86	2.58
	TMA	y = 1.0232x + 2.7232	0.9672	0.52	1.57
50M100C	Acetic acid	y = 1.0860x + 3.8948	0.8557	1.58	4.74
	Ammonia	y = 1.4774x + 3.0673	0.9458	2.33	7.00
	TMA	y = 1.1717x + 1.9025	0.9962	2.03	6.11

2.7. Indicator characterization

2.7.1. Scanning electron microscopy (SEM)

To obtain the microscopic images, the photo paper samples (i.e., blank and printed with indicator 100M100C) was attached to the conductive adhesive, which was then sprayed by platinum coating for 150 s. The coated samples were then observed under a scanning electron microscope (Hitachi SU8100, Schaumburg, IL, USA). Micrograms for the two different photo paper samples were captured with the magnification range of 500–3000.

2.7.2. Light and oxygen fastness

In order to evaluate the light and oxygen fastness of the printed indicators during storage, the three indicators were respectively placed under different conditions, whether stored at dark areas, and stored under vacuum or with direct exposure to the air. Specifically, these environmental conditions are denoted as: condition A (light and oxygen), condition B (light and vacuum), condition C (dark and vacuum), and condition D (dark and oxygen) at room temperature for 6 days. The change of corresponding $L^*/a^*/b^*$ values was recorded accordingly by a colorimeter (CR-410, Konika, Japan), and the Euclidean distance (ΔE) values are calculated for the comparison of total color changes. Under the $L^*a^*b^*$ system, L^* represents illuminance, ranging from 0 to 100; a^* represents redness to greenness, ranging from -120 to 120; and b^* for yellowness to blueness, ranging from -120 to 120. The overall color change was subsequently expressed as ΔE by Equation (5):

$$\Delta E = [(L_2 - L_1)^2 + (a_2 - a_1)^2 + (b_2 - b_1)^2]^{0.5} \quad (5)$$

where the subscripts “1” and “2” are the color values “before” and “after” detection, respectively.

2.8. Volatile gas detection

The pre-designed rectangular indicators were printed on glossy photo papers, with the original color parameters recorded by the colorimeter. The printed indicator was then attached to the interior of a clear plastic cup lid, where the total volume of the cup was 100 mL. To test their color responsiveness towards five different volatile gases (trimethylamine, ammonia, acetic acid, butyric acid, and hexanoic acid), each volatile gas sample was transferred into the container to reach with different concentrations, and the color parameters ($L^*a^*b^*$) before and after gas exposure were recorded by the colorimeter, with the calculation of total color changes (ΔE). All tests were conducted in four replicates. Based on our previous work (Luo and Lim, 2020b), the limit of detection (LOD) and limit of quantitation (LOQ) were calculated as previously described Equations (6) and (7):

$$\text{LOD} = 3.3 \sigma/S \quad (6)$$

$$\text{LOQ} = 10 \sigma/S \quad (7)$$

where σ is root-mean-square deviation and S is the slope of the fitted line of the calibration curve.

2.9. Preliminary study on shrimp freshness monitoring

In order to investigate the indicator’s performance in food packaging applications, a preliminary study was conducted on using the three indicators to monitor the deteriorative quality loss of fresh shrimps. For each testing cell, a whole fresh shrimp of uniform size (30 ± 5 g) was place in a sealed PET plastic container for 12 h at 20–22 °C. The indicator was fixed to the lid of the container, with the colored side facing upward direction for image capturing. The gradual color change for each indicator within 12 h was measured and recorded by the colorimeter.

2.10. Statistical analysis

Results were presented as mean \pm standard variation. The significant difference between color parameters was determined by analysis of variance (ANOVA) followed by Duncan test ($p < 0.05$). To differentiate the various color response amongst the volatile gases at same concentration, principal component analysis (PCA) and hierarchical cluster analysis (HCA) were performed. All the analyses were conducted by IBM SPSS Statistics 28 (IBM Corp., Armonk, NY, USA).

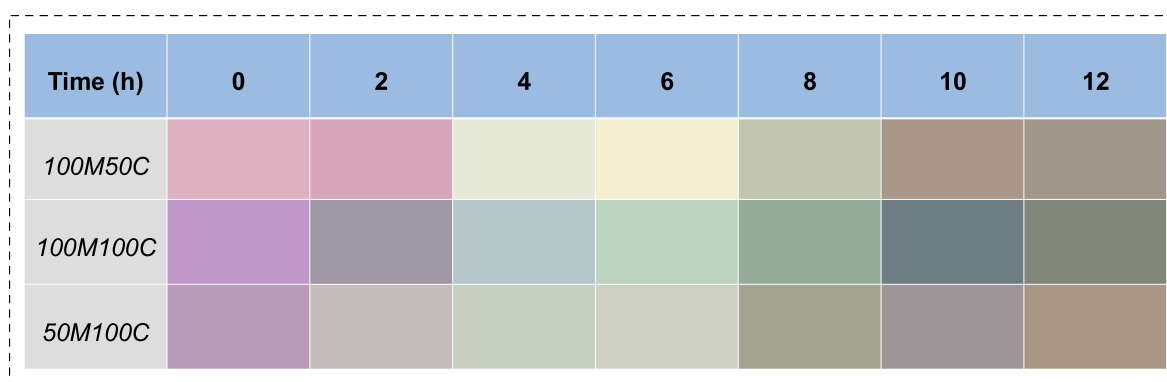


Fig. 8. Color responses of the three indicators towards the monitoring of whole shrimps stored at room temperature for 12 h.

3. Results and discussion

3.1. Pigment extraction and quantification

The betacyanin content from red pitaya peel extract was 4.45 mg/g dried fruit peel, and the anthocyanin content from grape peel extract was 3.42 mg/g dried fruit peel. Based on the printing ink formulation protocol described in Section 2.3, the betacyanin and anthocyanin concentration in the formulated ink was 2.24 mg/mL and 1.71 mg/mL respectively, representing significant amount of indicator colorants available for printing.

In general, ethanol and water can be selected for betacyanin extraction, but ethanol tends to precipitate the pectin. To this end, in our study, the addition of pectinase was implemented to help completely decompose the pectin into galacturonic acid, in order to improve the extraction efficiency (Qin et al., 2020), and reduce the impact on ink's rheological properties. Previous study states that grinding the fruit sample can improve the extraction efficiency (De Azeredo et al., 2009), while opposite results were reported by other previous literature studies as well as in the present study. It is speculated that grinding greatly increases the sample's surface area with increasing water retention during extraction. As a result, a modified procedure for betacyanin extraction was performed in the present study.

Anthocyanins are usually extracted with polar solvents, such as water, ethanol, and methanol (Silva et al., 2019). When anthocyanins are not bound to sugar (i.e., anthocyanin aglycones), they are more soluble in alcohol. In addition, anthocyanins in grape skin exist in various forms such as petunidin and malvidin. Compared with aqueous solution, ethanol solution can interact with more kinds of anthocyanins to improve the extraction efficiency (Musso et al., 2019). Nowadays the efficiency of anthocyanins extracted from grapes is usually within the range of 300–7500 mg/kg, and the value in the present study is 3420 mg/kg from grape peel, which is considered satisfactory.

3.2. Ink printability and pH sensitivity

3.2.1. Printable ink

Under the mechanism of DOD piezoelectric inkjet printing, when the ink flows to the printhead, the piezo element deforms to extrude the ink for stable drop generation (Derby, 2010). In order to ensure that the ink can be continuously and accurately jetted out, the force given by the piezoelectric device must be able to be larger than the friction and the surface tension of the ink at the print nozzle. Through tremendous simulation work by previous researchers, a printable region can be determined through the measurement of the density, dynamic viscosity, and surface tension of the ink, which are directly related to the Reynolds and Weber number. The commonly used Z value, which is the reciprocal of the Ohnesorge number, can be used to predict whether a prepared ink is printable fluid, where $1 < Z < 10$ represents the stable ink production region (Derby, 2010). Inks with high viscosity and low Z are difficult to be jetted, while inks with low surface tension and low Z value will lead to dripping problems. In contrast, inks with high Z value and low viscosity may lead to ink splashing (Luo and Lim, 2020a). The surface tension, dynamic viscosity, density, and Z values are shown in Table 1 below. Both formulated inks are exhibiting Newtonian behavior, and the derived Z values are between 4 and 6, demonstrating both the inks are printable fluid.

3.2.2. Ink pH sensitivity

The color appearance of the diluted red pitaya ink is similar to the samples adjusted to the pH range between 3 and 5, as shown in Fig. 1. With pH decrease, the red color of the liquid ink deepens, and the absorption peak of betacyanin at 538 nm becomes steeper, while the absorbance at 400 nm declines. As the alkalinity increases, the ink color gradually changes from red to yellow, becoming significantly bright yellowish at pH 13, while the absorption peak gradually shifts to the

wavelength of around 400 nm. The appearance of the new absorption peak is attributed to the degradation products of yellow betaxanthin and colorless cyclo-Dopa 5-*O*-(malonyl)- β -glucoside in alkaline environment (Khan, 2016). Through Fig. 1(C), it can be found that the addition of acetic and butyric acid can enhance the absorption at 500–550 nm, while TMA and ammonia causes the hypsochromic shift, which is consistent with the yellow color formation at high pH condition. Overall, the magenta reddish color of betacyanin was confirmed to be relatively stable at low to medium pH conditions or with the exposure to acids, but changed to yellowish with increased alkalinity or exposure to strong basic substances.

The colorimetric reaction of grape peel ink is dependent on the various pH conditions, with reversible color changes, due to the structural rearrangements during protonation or deprotonation, and changes in the total number of resonant electrons (Halonen et al., 2020). The color appearance of diluted anthocyanin ink is similar to the color of pH-adjusted samples at pH 4–5. With lower pH, the intensity of the red-color absorption at 510 nm increases, which is corresponding to the main isomer form of reddish flavylium, as shown in Fig. 2. When pH is in the range of 4–8, a mixture of different forms of anthocyanins are present, including the red flavylium and purple/blue quinoidal base, and yellow chalcone, resulting in the overall purplish color. When pH is higher than 9, chalcone becomes the predominant form with the maximum absorbance at 630 nm, imparting the yellowish coloration. Solution reaction with targeted acids and bases is the embodiment of pH change. For instance, acetic acid and butyric acid caused lower pH and deepened reddish color, whereas TMA and ammonia enhanced the alkalinity with ink's color changed to yellowish. Hexanoic acid are not miscible with water, so it was unable to determine the full spectral scan, even the similar acidic color response was observed.

3.3. Indicator characterization

Commercial piezoelectric inkjet printer possesses multiple nozzles at the printhead. Upon a printing demand is initiated, the ink is jetted out from the nozzle for firstly form a colored stream, which further breaks into drops and deposits onto the printing substrate. The SEM micrographs in Fig. 3 demonstrate that the blank photo paper surface with a sponge-like structure, which disappears significantly after ink deposition, consistent with our previous work when colorimetric inks were printed onto the surface of plastic film (Luo and Lim, 2020a). The print performance can be further improved, as shown by the printed ink "lines" in Fig. 3(B), which may be partially caused by the relatively slow solvent evaporation and ink spreading on photo paper surface.

Betacyanin and anthocyanin are photosensitive and thermosensitive, so their colors tend to fade with direct and long-time exposure to light and high temperature conditions (Etxabide et al., 2021). Considering the practical application scenarios of food packaging industry, the high-temperature storage conditions were not implemented in the current study. The overall color changes of the three printed indicators stored under conditions A–D are shown in Fig. 4. It can be seen that the indicators under light and oxygen exposure exhibited the highest degree of color change, while the ones stored under dark and vacuum condition showed the highest stability of least color change. Thus, it is recommended to store the printed natural colorant-based indicators in dark and low oxygen environment to retain its functionality. Further studies to enhance the indicator's stability can be considered, such as by printing a colorless inert ink as a protective layer, or attach a light/oxygen blocking material to increase the indicator ink's shelf-life.

3.4. Volatile gas detection

3.4.1. Volatile gas discrimination

The three-dimensional PCA plot and HCA dendrogram for volatile gas discrimination are presented in Fig. 5. As shown, the clusters of acetic acid, butyric acid, and hexanoic acid can be separated clearly,

with over 86 % discriminatory information (Fig. 5(A)). The clusters of TMA and ammonia are overlapping with each other in the PCA plot, due to their similar color-changing mechanisms. Amongst the five volatile gases tested, TMA exhibited the strongest color response and hexanoic acid showed the lowest reactivity to all indicators. From the HCA dendrogram (Fig. 5(B)), it can be seen that all individual gas analytes were classified correctly, demonstrating the satisfactory discriminatory capability based on the three indicators' color responses.

3.4.2. Comparison of different indicators' responses

For each gas analyte, the color response trend of the three indicators are similar. For example, the change of *L* fluctuates over the tested concentration range; the *a* value decreases with the increasing of TMA or ammonia concentration, while increases with more acetic acid exposure; and the color change of *b* value is opposite to the trend of *a* value (Fig. 6). Based on the overall color changes dictated by ΔE in Fig. 7, least color change was observed on indicator 100M/50C, while the indicator 100M/100C exhibited the highest degree of color change, as anticipated. The enhanced sensitivity of 100M/100C indicator may stem from the synergistic effect of the two pigments.

For the colorimetric detection of acetic acid, TMA, and ammonia, the three indicators exhibited distinct disparities in different color responses (see Table 2). The 100M/100C indicator showed the lowest LOD across all gases tested, revealing that this indicator can detect food spoilage at the relatively earlier stage, alerting consumers promptly to potential food deterioration. The 100M/50C indicator also possesses a relatively low LOD and LOQ value, but the slope of the standard curve is less steep than the other two, implying a less pronounced response to increasing gas concentrations. In comparison, the 50M/100C possesses a higher LOD value. Overall, the 100M/100C indicator through the printing of blended colorants in relatively higher levels showed the highest performance in terms of the LOD and LOQ values.

3.5. Preliminary study on shrimp spoilage

Fresh shrimp deteriorates mainly due to autolytic degradation, lipolytic oxidation, and microbial enumeration. The latter stage of deteriorative reactions generate various types of spoilage metabolites, such as biogenic amines, volatile amines, short-chain aldehydes and esters, peptides and amino acids, constituting the package headspace of spoiled shrimp (Luo et al., 2022; Odeyemi et al., 2018). The signature spoilage gases are mainly attributed to the volatile basic nitrogenous compounds that increase the alkalinity (Mehrzhad et al., 2024), so the indicators were expected to change towards the yellowish or brownish coloration. Fig. 8 shows the experimental color response of the three indicators to monitor shrimp freshness within 12 h. As expected, with longer storage time at room temperature, it can be seen that significant color changes were observed for all indicators tested. When the storage time exceeded 8 h, it was observed that the colors of the three indicators became slightly faded due to potential pigment degradation. Hence either considering enhancing the indicator's shelf-stability or switching the print substrate can be potential solutions to increase its practical application for long-term use under ambient environmental conditions.

4. Conclusions

In this study, betacyanin and anthocyanin were effectively extracted from fruit peels and the derived pigment concentrates were subsequently employed to develop colorimetric indicators via inkjet printing technology. The developed indicator inks were proved to be printable fluid and exhibited substantial pH sensitivity towards the exposure to different acidic or alkaline analytes. The results suggested that the inkjet-printed indicators composed of two natural colorants exhibited enhanced detection capabilities for acetic acid, TMA, and ammonia, and substantial color changes were captured for shrimp spoilage detection in a preliminary study. The inkjet-printed intelligent packaging materials

produced from fruit waste in the present study are promising for the development of future commercial packaging designs. Future research endeavors can be made to enhance the indicator's shelf stability of inkjet-printed natural colorants, to explore the detection limit of other food spoilage analytes, and to systematically study the food packaging applications by building the predictive models based on the color responses and food deteriorative reaction parameters.

CRedit authorship contribution statement

Tianxi Gong: Methodology, Software, Validation, Formal analysis, Data curation, Writing – original draft. **Xiaoyu Luo:** Conceptualization, Investigation, Resources, Supervision, Project administration, Funding acquisition, Writing – review & editing.

Declaration of competing interest

The authors have no conflict of interest to be declared.

Acknowledgements

The present study is supported by the research grants from the National Natural Science Foundation of China (grant number: 32350410396) and Beijing Normal–Hong Kong Baptist University, Zhuhai, China (project code: UICR0300025).

Data availability

Data will be made available on request.

References

- André, S., Vallaes, T., Planchon, S., 2017. Spore-forming bacteria responsible for food spoilage. *Res. Microbiol.* 168 (4), 379–387. <https://doi.org/10.1016/j.resmic.2016.10.003>.
- Chen, H., Zhang, M., Bhandari, B., Yang, C., 2020. Novel pH-sensitive films containing curcumin and anthocyanins to monitor fish freshness. *Food Hydrocoll.* 100, 105438. <https://doi.org/10.1016/j.foodhyd.2019.105438>.
- Cheng, H., Xu, H., Julian McClements, D., Chen, L., Jiao, A., Tian, Y., Miao, M., Jin, Z., 2022. Recent advances in intelligent food packaging materials: principles, preparation and applications. *Food Chem.* 375, 131738. <https://doi.org/10.1016/j.foodchem.2021.131738>.
- De Azeredo, H.M.C., Pereira, A.C., De Souza, A.C.R., Gouveia, S.T., Mendes, K.C.B., 2009. Study on efficiency of betacyanin extraction from red beetroots. *Int. J. Food Sci. Technol.* 44 (12), 2464–2469. <https://doi.org/10.1111/j.1365-2621.2009.02037.x>.
- Derby, B., 2010. Inkjet printing of functional and structural materials: fluid property requirements, feature stability, and resolution. *Annu. Rev. Mater. Res.* 40, 395–414. <https://doi.org/10.1146/annurev-matsci-070909-104502>.
- Etxabide, A., Kilmartin, P.A., Maté, J.I., 2021. Color stability and pH-indicator ability of curcumin, anthocyanin and betanin containing colorants under different storage conditions for intelligent packaging development. *Food Control* 121, 107645. <https://doi.org/10.1016/j.foodcont.2020.107645>.
- Fernández-Ramos, M.D., Pageo-Cabrera, M., Capitán-Vallvey, L.F., Pérez de Vargas-Sansalvador, I.M., 2021. Inkjet-printed O₂ gas sensors in intelligent packaging. *Analyst* 146 (10), 3177–3184. <https://doi.org/10.1039/D1AN00295C>.
- Fu, Y., Shi, J., Xie, S.-Y., Zhang, T.-Y., Soladoye, O.P., Aluko, R.E., 2020. Red beetroot betalains: perspectives on extraction, processing, and potential health benefits. *J. Agric. Food Chem.* 68 (42), 11595–11611. <https://doi.org/10.1021/acs.jafc.0c04241>.
- Halonen, N., Pálvölgyi, P.S., Bassani, A., Fiorentini, C., Nair, R., Spigno, G., Kordas, K., 2020. Bio-based smart materials for food packaging and sensors – a review. *Front. Mater.* 7. <https://doi.org/10.3389/fmats.2020.00082>.
- Herbach, K.M., Stintzing, F.C., Carle, R., 2006. Betalain stability and degradation—structural and chromatic aspects. *J. Food Sci.* 71 (4). <https://doi.org/10.1111/j.1750-3841.2006.00022.x>.
- Kalpana, S., Priyadarshini, S.R., Maria Leena, M., Moses, J.A., Anandharamakrishnan, C., 2019. Intelligent packaging: trends and applications in food systems. *Trends Food Sci. Technol.* 93, 145–157. <https://doi.org/10.1016/j.tifs.2019.09.008>.
- Khan, M.I., 2016. Stabilization of betalains: a review. *Food Chem.* 197, 1280–1285. <https://doi.org/10.1016/j.foodchem.2015.11.043>.
- Kossyvakli, D., Contardi, M., Athanassiou, A., Fragouli, D., 2022. Colorimetric indicators based on anthocyanin polymer composites: a review. *Polymers* 14 (19), 4129. <https://doi.org/10.3390/polym14194129>.
- Luo, X., 2022. Application of inkjet-printing technology in developing indicators/sensors for intelligent packaging systems. *Curr. Opin. Food Sci.* 46, 100868. <https://doi.org/10.1016/j.cofs.2022.100868>.

- Luo, X., Lim, L.-T., 2020a. An inkjet-printed sulfonephthalein dye indicator array for volatile amine detection. *J. Food Sci.* 85 (2), 442–454. <https://doi.org/10.1111/1750-3841.15020>.
- Luo, X., Lim, L.-T., 2020b. Curcumin-loaded electrospun nonwoven as a colorimetric indicator for volatile amines. *Lebensm. Wiss. Technol.* 128, 109493. <https://doi.org/10.1016/j.lwt.2020.109493>.
- Luo, X., Ho, I., Brankovan, S., Lim, L.-T., 2021. Inkjet-printed gradient colorimetric indicators for monitoring fish freshness. *Food Packag. Shelf Life* 29, 100719. <https://doi.org/10.1016/j.fpsl.2021.100719>.
- Luo, X., Zaitoon, A., Lim, L.-T., 2022. A review on colorimetric indicators for monitoring product freshness in intelligent food packaging: indicator dyes, preparation methods, and applications. *Compr. Rev. Food Sci. Food Saf.* 21 (3), 2489–2519. <https://doi.org/10.1111/1541-4337.12942>.
- Mehrzdad, A., Verdian, A., Sarabi-Jamab, M., 2024. Smart nano-inks based on natural food colorant for screen-printing of dynamic shelf life of shrimp. *Food Chem.* 447, 138963. <https://doi.org/10.1016/j.foodchem.2024.138963>.
- Musso, Y.S., Salgado, P.R., Mauri, A.N., 2019. Smart gelatin films prepared using red cabbage (*Brassica oleracea* L.) extracts as solvent. *Food Hydrocoll.* 89, 674–681. <https://doi.org/10.1016/j.foodhyd.2018.11.036>.
- Odeyemi, O.A., Burke, C.M., Bolch, C.C.J., Stanley, R., 2018. Seafood spoilage microbiota and associated volatile organic compounds at different storage temperatures and packaging conditions. *Int. J. Food Microbiol.* 280, 87–99. <https://doi.org/10.1016/j.ijfoodmicro.2017.12.029>.
- Pacquit, A., Frisby, J., Diamond, D., Lau, K., Farrell, A., Quilty, B., Diamond, D., 2007. Development of a smart packaging for the monitoring of fish spoilage. *Food Chem.* 102 (2), 466–470. <https://doi.org/10.1016/j.foodchem.2006.05.052>.
- Patel, S., Shrivastava, K., Sinha, D., Monisha, Kumar Patle, T., Yadav, S., Thakur, S.S., Deb, M. K., Pervez, S., 2022. Smartphone-integrated printed-paper sensor designed for on-site determination of dimethoate pesticide in food samples. *Food Chem.* 383, 132449. <https://doi.org/10.1016/j.foodchem.2022.132449>.
- Phan Van, M., Tran Duc, D., Thi Thanh, H.D., Chi, H.T., 2020. Comparison of ultrasound assisted extraction and enzyme assisted extraction of betacyanin from red dragon fruit peel. *E3S Web of Conferences* 187, 04004. <https://doi.org/10.1051/e3sconf/202018704004>.
- Qin, Y., Liu, Y., Zhang, X., Liu, J., 2020. Development of active and intelligent packaging by incorporating betalains from red pitaya (*Hylocereus polyrhizus*) peel into starch/polyvinyl alcohol films. *Food Hydrocoll.* 100, 105410. <https://doi.org/10.1016/j.foodhyd.2019.105410>.
- Robertson, G.L., 2016. *Food Packaging*. CRC Press. <https://doi.org/10.1201/b21347>.
- Rodríguez-Mena, A., Ochoa-Martínez, L.A., González-Herrera, S.M., Rutiaga-Quiñones, O.M., González-Laredo, R.F., Olmedilla-Alonso, B., 2023. Natural pigments of plant origin: classification, extraction and application in foods. *Food Chem.* 398, 133908. <https://doi.org/10.1016/j.foodchem.2022.133908>.
- Saichana, N., Matsushita, K., Adachi, O., Frébort, I., Frébortova, J., 2015. Acetic acid bacteria: a group of bacteria with versatile biotechnological applications. *Biotech. Adv.* 33 (6), 1260–1271. <https://doi.org/10.1016/j.biotechadv.2014.12.001>.
- San-Valero, P., Fernández-Naveira, Á., Veiga, M.C., Kennes, C., 2019. Influence of electron acceptors on hexanoic acid production by *Clostridium kluyveri*. *J. Environ. Manag.* 242, 515–521. <https://doi.org/10.1016/j.jenvman.2019.04.093>.
- Silva, C. K. da, Mastrantonio, D.J. da S., Costa, J.A.V., Morais, M. G. de, 2019. Innovative pH sensors developed from ultrafine fibers containing açai (*Euterpe oleracea*) extract. *Food Chem.* 294, 397–404. <https://doi.org/10.1016/j.foodchem.2019.05.059>.
- Soni, S., Sathe, P., Sarkar, S.K., Kushwaha, A., Gupta, D., 2024. Inkjet-printed sub-zero temperature sensor for real-time monitoring of cold environments. *Int. J. Biol. Macromol.* 258, 128774. <https://doi.org/10.1016/j.ijbiomac.2023.128774>.
- Stafford, H.A., 1994. Anthocyanins and betalains: evolution of the mutually exclusive pathways. *Plant Sci.* 101 (2), 91–98. [https://doi.org/10.1016/0168-9452\(94\)90244-5](https://doi.org/10.1016/0168-9452(94)90244-5).
- Tasangong, B., Henry, C.S., Sameenoi, Y., 2023. Diameter-based inkjet-printed paper devices for formaldehyde analysis in foods. *Food Control* 145, 109408. <https://doi.org/10.1016/j.foodcont.2022.109408>.
- Yam, K.L., Takhistov, P.T., Miltz, J., 2005. Intelligent packaging: concepts and applications. *J. Food Sci.* 70 (1), R1–R10. <https://doi.org/10.1111/j.1365-2621.2005.tb09052.x>.
- Yu, D., Cheng, S., Li, Y., Su, W., Tan, M., 2024. Recent advances on natural colorants-based intelligent colorimetric food freshness indicators: fabrication, multifunctional applications and optimization strategies. *Crit. Rev. Food Sci. Nutr.* 64 (33), 12448–12472. <https://doi.org/10.1080/10408398.2023.2252904>.
- Zhang, Y., Lim, L.-T., 2016. Inkjet-printed CO₂ colorimetric indicators. *Talanta* 161, 105–113. <https://doi.org/10.1016/j.talanta.2016.08.014>.